A Two-Structure Model of Thermodynamic Properties and Surface Tension of Supercooled Water

Jan Hrubý[1*] and Vincent Holten [2]

[1] Institute of Thermomechanics AS CR, Dolejškova 5, CZ-182 00 Prague 8, Czech Rep.
[2] Eindhoven University of Technology, Department of Applied Physics, P.O. Box 513, 5600 MB, Eindhoven, The Netherlands
[*]E-mail: hruby@it.cas.cz

A thermodynamic model was developed describing the liquid and gaseous phases of water. The model correctly represents the strong anomalous behavior of supercooled water. The anomalies are due to the vicinity of liquid-liquid critical point. This interpretation differs from the IAPWS-95 formulation, where the anomalies are attributed to liquid-to-gas spinodal, re-entering the region of positive pressures. Unlike IAPWS-95, the present model can be used for extrapolation of thermodynamic properties to low temperatures. The model approximates liquid water as a mixture of two competing structures (high- and low-density structure) and cavities. The thermodynamic state is found by minimizing the Gibbs free energy with respect to the proportion of the two structures and number of cavities. The mixture approach is further used to model the surface tension.

1. Introduction

Recent measurements of homogeneous nucleation rates in water vapor [1-3] indicate that the critical clusters (droplets of radius ~1 nm) are liquid in the experimental range, extending down to 205 K. Light scattering experiments show that most probably they remain liquid during rapid growth (within 10-100 ms) up to the micrometer size. To analyze the processes of nucleation and growth of such nano-droplets, knowledge of thermophysical properties of supercooled water is required. This need encouraged us to develop a thermodynamic model of water, giving a consistent explanation of the anomalous behavior of density, specific heat, surface tension, and related properties of supercooled water.

Perhaps the most plausible hypothesis [4], explaining the huge anomalous effects in supercooled water is that at low temperatures, two liquid phases can exist: the Low Density Liquid (LDL), and the High Density Liquid (HDL). The phase separation occurs below the second (liquid-liquid) critical point of water. Below the glass transition temperature, LDL/HDL become low/high density amorphous ices (LDA/HDA). This behavior is in contrast with the IAPWS-95 formulation by Wagner and Pruß [5], where the liquid-vapor spinodal re-enters the region of positive pressure at

low temperatures, giving rise to the anomalies. We consider such behavior as unphysical; if the liquid would be quenched sufficiently fast to prevent freezing, it should evaporate when crossing the spinodal. This is, indeed, not true; quenched liquid becomes amorphous ice.

The present model is based on an idea suggested already by Röntgen [6] in 1892: liquid water is assumed to consist of two nanoscopic structures. The anomalous behavior is due to the change of the proportion of these structures. This is, indeed, an approximation.

2. Discussion of Existing Experimental Data

Experimental data for density, isobaric heat capacity, and speed of sound in supercooled water exist only at atmospheric pressure and in a limited temperature range (down to 236 K). A detailed review of existing data is given in Ref. [5]. The IAPWS-95 formulation represents accurately the density measurements and the heat capacity (there is a slight disagreement with a newer dataset by Archer and Carter [7]). IAPWS-95 fails in representing speed of sound at sub-zero temperatures. Wagner and Pruß concluded "the speed-of-sound data of Trinh and Apfel [8] and Petitet et al. [9] are not consistent with the $p\rho T$ data of Kell [10] and of Hare and Sorensen [11]". We do

not agree with this conclusion: the mentioned density data are only at atmospheric pressure (no information on compressibility). Therefore, it is impossible to compute speed of sound out of the density and heat capacity measurements, which could be compared with direct experimental measurements of speed of sound.

We found only three datasets for the surface tension of supercooled water. The oldest [12] gives only two datapoints. The data by Hacker seems to be of exceptional quality [13]. Until recently, this data was not known to researchers, including Floriano and Angell [14], authors of the latest data. The data by Hacker shows much less scatter, contains by an order of magnitude more datapoints and are well documented. The data by Floriano and Angel seem to indicate a dependency of apparent surface tension on the capillary diameter. This effect may be of common origin with dependency of apparent density on capillary diameter, observed by Hare and Sorensen [11].

3. Model for Thermodynamic Properties of Water in Liquid and Gaseous phases

The model is based on the following approximate theoretical concept. The system can be divided into cells. Each cell contains one water molecule or it is empty. The water molecule can be a member of either the low-density structure (LDS) or the high-density structure (HDS). With subscript 1 and 2 we denote cells, containing LDS and HDS members, respectively. Subscript 3 will denote empty cells. The respective numbers of cells in the system are N_1, N_2, and N_3. The total number of molecules is $N=N_1+N_2$, and the total number of cells is $K=N_1+N_2+N_3$. We introduce *structural fractions*

$$x_k \equiv N_k / N , \quad k=1,2,3 . \tag{1}$$

Clearly it holds

$$x_1 + x_2 = 1 , \quad \Sigma x \equiv x_1 + x_2 + x_3 = 1 + x_3 . \tag{2}$$

The number of configurations of the system for given N_1, N_2, and N_3 is

$$B_3 = \frac{K!}{N_1! N_2! N_3!} . \tag{3}$$

The membership in one of the structures is determined by interaction with molecules in neighboring cells. Therefore, in the absence of interactions – in the ideal gas state – the

membership cannot be determined. Therefore, in the gas phase the number of configurations is only

$$B_2 = \frac{K!}{N! N_3!} . \tag{4}$$

We assume that the effective number of configurations can be estimated by interpolation

$$B \approx B_3^{N/K} B_2^{1-(N/K)} . \tag{5}$$

Consequently, the specific ideal mixing entropy is

$$s_{\text{imix}}(\mathbf{x}) = R \frac{\ln B}{N}$$
$$= R \left(-\frac{x_1 \ln x_1 + x_2 \ln x_2}{\Sigma x} - x_3 \ln x_3 + \Sigma x \ln \Sigma x \right) . \tag{6}$$

The Stirling's formula was used to obtain the last result.

The mean potential energy is estimated conventionally as

$$U = \frac{1}{2} \sum_{k=1}^{2} N_k \sum_{l=1}^{2} n_{kl} U_{kl} , \tag{7}$$

where U_{kl} is interaction energy of neighboring cells of types k and l, and n_{kl} is average number of l-type neighbors of k-type cell. The summation does not include empty cells: the pairs including one or two emty cells do not contribute ($U_{13}=U_{23}=U_{33}=0$). Using the random mixing approximation we obtain

$$n_{kl} \approx \frac{n x_l}{\Sigma x} , \tag{8}$$

where n is total number of neighboring cells. The specific potential energy can then be written as

$$u = u_1 + x_2 \Delta u + \sum_{k=1}^{2} \sum_{l=k+1}^{3} \frac{x_k x_l}{\Sigma x} u_{kl} , \tag{9}$$

where u_1 is that of pure LDS ("component" 1), and Δu is the difference in the specific potential energy between pure HDS and LDS:

$$u_1 = \frac{n U_{11}}{2M} , \quad \Delta u = \frac{n}{2M} (U_{22} - U_{11}) . \tag{10}$$

Consequently, the cross terms are

$$u_{12} = \frac{n}{M} \left(U_{12} - \frac{U_{11} + U_{22}}{2} \right) ,$$
$$u_{13} = -\frac{n}{M} U_{11} , \quad u_{23} = -\frac{n}{M} U_{22} . \tag{11}$$

Further we assume that the cell volume, the effective number of degrees of freedom, and their excitation depends on the occupation of the given cell and can be influenced by neighbors. These considerations lead to the general form for the specific Gibbs free energy

$$g(p,T,\mathbf{x}) = g_1 + x_2\Delta g + x_3 g_3 - Ts_{\text{imix}}$$

$$+ \sum_{k=1}^{2}\sum_{l=k+1}^{3}\frac{x_k x_l}{\Sigma x}g_{kl}, \qquad (12)$$

$$g_1(p,T) = g_{1,0}(T) + \int_0^p v_1(p',T)\,\mathrm{d}p', \qquad (13)$$

$$g_3(p,T) = \int_0^p v_3(p',T)\,\mathrm{d}p', \qquad (14)$$

$$\Delta g(p,T) = \Delta u - T\Delta s - T(\ln T - 1)\Delta c$$

$$+ \int_0^p \Delta v(p',T)\,\mathrm{d}p', \qquad (15)$$

$$g_{kl}(p,T) = u_{kl} - Ts_{kl} - T(\ln T - 1)c_{kl}$$

$$+ \int_0^p v_{kl}(p',T)\,\mathrm{d}p'. \qquad (16)$$

In this model, Δu, Δs, Δc, u_{kl}, s_{kl}, and c_{kl} are considered as constants. The volume terms Δu, and v_{kl} are considered (generally) as functions of temperature and pressure.

A thermodynamic phase ϕ is determined by local minimum of the Gibbs free energy with respect to x_2 and x_3. The necessary condition is

$$\left.\frac{\partial g(p,T,\mathbf{x})}{x_2}\right|_\phi = 0, \quad \left.\frac{\partial g(p,T,\mathbf{x})}{x_3}\right|_\phi = 0. \quad (17)$$

The present model describes three phases: gaseous (G), low- and high-density liquids (LDL and HDL, respectively). The global minimum (lowest local minimum) represents thermodynamically stable phase. If two minima are equal, we have equilibrium coexistence of two phases. Equality of three minima represents triple point. It has to be kept in mind that supercooled phases LDL and HDL are metastable with respect to crystalline ice, which is not described by the present formulation.

Solving Eq. (17) for a number of conditions (p,T), we obtain functions $x_{\phi 2}(p,T)$ and $x_{\phi 3}(p,T)$. Substitution to Eq. (12) then gives ordinary Gibbs free energy for given phase, $g_\phi(p,T)$. We use the following notation:

$$y_{(p)} \equiv \left.\frac{\partial y(p,T,x_2,x_3)}{\partial p}\right|_\phi, \quad y_{(T)} \equiv \left.\frac{\partial y(p,T,x_2,x_3)}{\partial T}\right|_\phi,$$

$$y_{(k)} \equiv \left.\frac{\partial y(p,T,x_2,x_3)}{\partial x_k}\right|_\phi, \quad k = 2,3, \qquad (18)$$

$$y_{\phi(p)} \equiv \frac{\partial y_\phi(p,T)}{\partial p}, \quad y_{\phi(T)} \equiv \frac{\partial y_\phi(p,T)}{\partial T}. \quad (19)$$

Derivative of a property y of the thermodynamic phase ϕ with respect to pressure or temperature is obtained as

$$y_{\phi(p/T)} = y_{(p/T)} + \sum_{k=2,3} y_{(k)} x_{\phi k(p/T)}. \qquad (20)$$

We will call the two parts as *frozen* (change at constant-frozen $\mathbf{x}$) and *structural* (change at constant p, T). Volume and entropy are obtained as

$$v_\phi = g_{\phi(p)} = g_{(p)}, \quad s_\phi = -g_{\phi(T)} = -g_{(T)}. \quad (21)$$

The structural part vanishes here because of Eq. (17). From Eq. (12) we have volume

$$v(p,T,\mathbf{x}) = \sum_{k=1}^{3} x_k v_k(p,T) + \sum_{k=1}^{2}\sum_{l=k+1}^{3}\frac{x_k x_l}{\Sigma x}v_{kl}(p,T), \quad (22)$$

where $v_2 = v_1 + \Delta v$, and entropy

$$s(p,T,\mathbf{x}) = -\frac{\mathrm{d}\,g_{10}}{\mathrm{d}T} + x_2\left(\Delta s + \Delta c \ln T - \int_0^p \frac{\mathrm{d}\,\Delta v}{\mathrm{d}T}\,\mathrm{d}p'\right)$$

$$+ s_{\text{imix}} + \sum_{k=1}^{2}\sum_{l=k+1}^{3}\frac{x_k x_l}{\Sigma x}\left(s_{kl} + c_{kl}\ln T - \int_0^p \frac{\mathrm{d}\,v_{kl}}{\mathrm{d}T}\,\mathrm{d}p'\right). (23)$$

Condition Eq. (17) can be written as

$$g_{(k)} = 0, \qquad k = 2,3. \qquad (24)$$

We consider an infinitesimal change of temperature and pressure, during which a phase ϕ is retained, i.e. condition (24) is satisfied both in initial and final states. By differentiation of Eq. (24) we have

$$\sum_{l=2,3} g_{(k,l)}\,\mathrm{d}x_l = -g_{(k,p)}\,\mathrm{d}p - g_{(k,T)}\,\mathrm{d}T, \quad k = 2,3. \quad (25)$$

From this equation we find the derivatives

$$x_{\phi k(p)} = \frac{g_{(k,m)}v_{(m)} - g_{(m,m)}v_{(k)}}{g_{(22)}g_{(33)} - g_{(23)}g_{(32)}}, \quad \begin{array}{l}k = 2,3,\\ m = 5-k,\end{array} \quad (26)$$

$$x_{\phi k(T)} = -\frac{g_{(k,m)}s_{(m)} - g_{(m,m)}s_{(k)}}{g_{(22)}g_{(33)} - g_{(23)}g_{(32)}}, \quad \begin{array}{l}k = 2,3,\\ m = 5-k.\end{array} \quad (27)$$

For isobaric heat capacity c_p, compressibility κ_T, and expansion coefficient α, the structural parts do not vanish:

$$c_p = T s_{\phi(T)} = T\left(s_{(T)} + \sum_{k=2,3} s_{(k)} x_{\phi k(T)}\right), \quad (28)$$

$$\kappa_T = -v^{-1} v_{\phi(p)} = -v^{-1}\left(v_{(p)} + \sum_{k=2,3} v_{(k)} x_{\phi k(p)}\right), (29)$$

$$\alpha = v^{-1} v_{\phi(T)} = v^{-1}\left(v_{(T)} + \sum_{k=2,3} v_{(k)} x_{\phi k(T)}\right). \quad (30)$$

Equivalently,

$$\alpha = -v^{-1} s_{\phi(p)} = -v^{-1}\left(s_{(p)} + \sum_{k=2,3} s_{(k)} x_{\phi k(p)}\right). (31)$$

4. Ideal gas limit

If the number of vacant cells is much larger than the number of particles ($x_3 \square 1$), the Gibbs function Eq. (12) reduces to

$$g_\infty = g_{1,0} + g_{13,0} + x_3 g_{3,0} - RT(1 + \ln \Sigma x)$$
$$+ x_2\left(\Delta g_0 - g_{13,0} + g_{23,0}\right). \quad (32)$$

As already discussed, in the gas phase thermodynamics must be independent of x_2, because no distinction exists between HDS and LDS members. Therefore, we require

$$\Delta g_0 - g_{13,0} + g_{23,0} = 0. \quad (33)$$

This condition must hold for all temperatures in the range of low pressures. Therefore, we have

$$\Delta u - u_{13} + u_{23} = 0, \quad (34)$$

$$\Delta s - s_{13} + s_{23} = 0, \quad (35)$$

$$\Delta c - c_{13} + c_{23} = 0, \quad (36)$$

$$\Delta v_0 - v_{13,0} + v_{23,0} = 0, \quad (37)$$

where

$$\Delta v_0 \equiv \lim_{p\to 0} \Delta v, \quad v_{kl,0} \equiv \lim_{p\to 0} v_{kl}. \quad (38)$$

Eq. (34) follows already from relations (11). In addition, we will require that the cell volume for $x_3 \square 1$ is independent of its occupancy. This requirement follows from the fact that the dilatation of the cell volume is result of interactions with molecules in neighboring cells. If these are empty, the volume of occupied cell should be equal to empty cell volume. This provides a further relation:

$$v_{1,0} + v_{13,0} = v_{3,0}. \quad (39)$$

From this equation and Eq. (37) it follows that

$$v_{2,0} + v_{23,0} = v_{3,0}. \quad (40)$$

Applying condition (17) at state where $x_3 \square 1$, we obtain

$$\Sigma x = 1 + x_3 = \frac{RT}{pv_3}. \quad (41)$$

Taking into account Eqs. (32) to (41), we obtain the ideal gas Gibbs free energy

$$g_{id}(p,T) = g_{1,0}(T) + u_{13} - Ts_{13} - T(\ln T - 1)c_{13}$$
$$+ RT \ln \frac{pv_3}{RT}. \quad (42)$$

By differentiation we obtain

$$s_{id} = -\frac{\partial g_{id}}{\partial T} = -\frac{dg_{1,0}}{dT} + s_{13} + c_{13}\ln T + R$$
$$-R\ln\frac{pv_{3,0}}{RT} - R\frac{d\ln v_{3,0}}{d\ln T}, \quad (43)$$

$$c_{p,id} = T\frac{\partial s_{id}}{\partial T} = -T\frac{d^2 g_{1,0}}{dT^2} + c_{13} + R$$
$$-R\frac{d\ln v_{3,0}}{d\ln T} - R\frac{d^2\ln v_{3,0}}{d(\ln T)^2}. \quad (44)$$

The last equation is used to determine the function $g_{1,0}(T)$:

$$g_{1,0} = K_0 + K_1 T - \int_{T_t}^{T}\left[\int_{T_t}^{T''}\frac{c_{p,id}(T')}{T'}dT'\right]dT''$$
$$+(c_{13} + R)T(\ln T - 1) - RT\ln v_{3,0}(T), \quad (45)$$

where T_t is a reference temperature. In accord with IAPWS-95 formulation, the state is chosen as the liquid state of water at triple point ($T_t = 273.16$ K, $p_t = 611.655$ Pa). The constants K_0 and K_1 are determined in order that entropy and internal energy at the reference state vanish: $s_{L,t} = 0$, $u_{L,t} = g_{L,t} + T_t s_{L,t} + p_t v_{L,t} = 0$ (note that u denotes internal energy here, not potential interaction energy).

5. Fitting of the Model Parameters

The thermodynamic model contains a number of parameters, enabling its fitting to experimental data.

Table 1. Parameters of equation (46) for the specific volume of ice Ih. The values are valid for volume in m^3 kg^{-1} and temperature in K.

a_1	1.21779E-03
a_2	-4.33629E-05
a_3	4.38031E-06
a_4	-1.46258E-04
a_5	-9.88480E-06
a_6	5.58300E+01

Optimally, multi-property fitting should be used. This has not been achieved yet. On the way to the complete formulation, we first developed a simplified model, in which we assumed $\Delta s_{12}=\Delta c_{12}=0$ and $v_{12}=0$. The volumes v_1 and v_2 were assumed incompressible. The cavity volume v_3 was taken as $(v_1+v_2)/2$. We assumed that LDS is similar on the local scale to the hexagonal ice Ih. Therefore, we approximate $v_1 \approx v_{Ih}$. Based on the measurements of lattice constants by Röttger *et al.* [15], we developed an equation for the specific volume of Ih at normal pressure p_n=101325 Pa, valid down to 0 K and extrapolable to T>273.15:

$$v_{Ih} = a_1 + a_2 t \left(1 - y - ty\right) + a_3 t^2 \left(1-y\right)$$
$$+ a_4 \left(1 + t + \frac{1}{2}t^2\right) y + a_5 t^3 y , \qquad (46)$$

where $t \equiv T / a_6$ and $y \equiv \exp(-t)$. The parameters are given in Table 1.

Table 2. Parameters of Eqs. (12), (47), (48).

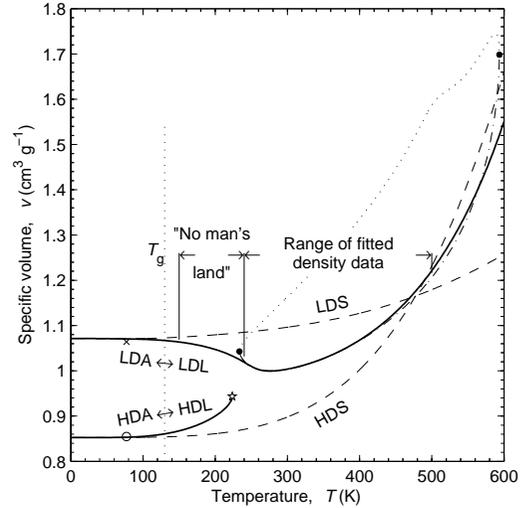|		
Δu	J kg^{-1}	3491.63
u_{12}	J kg^{-1}	224514.7
u_{13}	J kg^{-1}	3087200
s_{13}	J kg^{-1} K^{-1}	16635.7
c_{13}	J kg^{-1} K^{-1}	2359.75
R	J kg^{-1} K^{-1}	461.51805
b_1	m^{3}kg^{-1}	8.5266e-4
b_2	K	607.66
b_3	1	4.1571
P_{LDS}	1	52.9316
P_{HDS}	1	39.4034
n	1	4.511
c_1	N m^{-1}	1e-3
c_2	kg m^{-3}	18015.268

Fig. 1. Specific volume of liquid and amorphous water at 101325 Pa. Solid lines: liquid and amorphous phases predicted by the present model. Dash-dotted and dotted lines: Ref. [5]. Cross and open circle: measurements for LDA and HDA, respectively. Star: HDL-LDL spinodal point. Solid circles: liquid-vapor spinodal points. T_g: glass transition temperature.

An empirical equation is assumed for HDS:
$$v_{HDS,n} / b_1 = 1 + (T / b_2)^{b_3} . \qquad (47)$$

Parameters b_1, b_2, b_3, Δu, and u_{12} have been obtained by fitting liquid densities [5] at normal pressure p_n =101325 Pa in the range 240-500 K, with x_3 set to 0 (the influence of cavities on liquid density is significant above 400 K). Then parameters u_{13}, s_{13}, and c_{13} were fitted to the saturated vapor pressure in range 273.16-298 K. We chose this narrow interval in order to prevent influence of gas phase non-ideality—we assume that the present model (similarly to cubic equations) is not particularly good for describing vapor non-ideality. Values of the parameters are given in Table 2. Results are shown at Fig. 1. At p_n below 223 K the model predicts two liquid phases, the more stable (higher g) low-density liquid (LDL) and the high-density liquid (HDL). It is assumed [4] that they transform into the low-density amorphous ice (LDA) and high-density amorphous ice (HDA), respectively, at glass temperature $T_g \cdot$ 130 K. Interestingly, the experimental densities of LDA (cross) and HDA (open circle) at 77 K are predicted accurately.

6. Surface Tension

Considering liquid water as a mixture of "components" LDS and HDS, the surface tension can be described with the Macleod-Sugden correlation [16], adapted into the form

$$\sigma(T, x_1)/c_1 = \left[\mathbf{P}(x_1)/ c_2 v(T, x_1) \right]^n. \quad (48)$$

Here, c_1 and c_2 are constants ensuring dimensional consistency, and $\mathbf{P}$ is the *parachor*:

$$\mathbf{P}(x_1) = (1 - x_1)\mathbf{P}_{LDS} + x_1\mathbf{P}_{HDS}. \quad (49)$$

The pure-component parachors $\mathbf{P}_{LDS}$ and $\mathbf{P}_{HDS}$, and the exponent n, were found by fitting surface tension data by Hacker for 251-273 K and the IAPWS formula [17,18] for 273-373 K. The results are shown at Fig. 2.
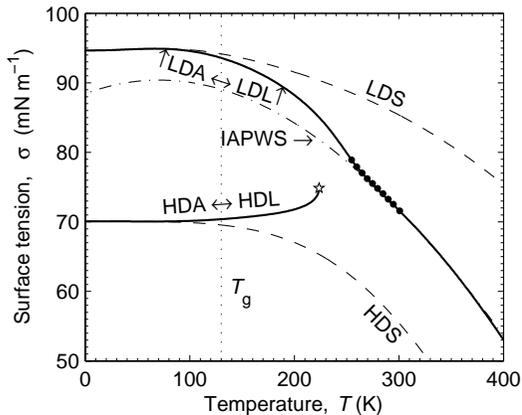

Fig. 2. Surface tension of liquid and amorphous water. Solid lines: Eq.(48). Dots: Ref. [13]. The experimental data shows an almost sudden change of slope, which is well reproduced by the model. Also shown is prediction of surface tension of the high-density liquid (HDL).

7. Conclusions

A thermodynamic model was developed, enabling a plausible extrapolation of thermodynamic properties of water deep into the supercooled region. Below 223 K, the model predicts existence of a second, denser, liquid phase. This behavior is in accord with hypotheses given in literature [4]. In this work we present preliminary values of the model parameters. With these values, the model accurately describes densities and the saturated vapor pressure. The anomalous

enhancement of isobaric heat capacity of supercooled water is underestimated. Very little testing has been done for the behavior at elevated pressures. As a next step, the model parameters (a number of them were set zero here) should be found by multi-property fitting. The behavior of the model is to some extent analogous to the cubic equations of state. It produces the "Van der Waals loop" of isotherms. Therefore, it may prove useful for computations, where such behavior is required, i.e. gradient theory of phase interface.

References and Notes
[1] J. Wölk and R. Strey, *J. Phys. Chem. B*, **105,** 11683 (2001).
[2] P. Peeters, J. J. H. Gielis, and M. H. H. van Dongen, M. E. H., *J. Chem. Phys.*, **117,** 5647 (2002).
[3] D. G. Labetski, V. Holten, and M. E. H. van Dongen, *J. Chem. Phys.*, **120,** (2004), to be published.
[4] O. Mishima and H.E. Stanley, *Nature*, **396**, 329 (1998)
[5] W. Wagner and A Pruß, *J. Phys. Chem. Ref. Data*, **31,** 387 (2002).
[6] W. C. Röntgen, *Ann. Phys. Chem.*, **45**, 91 (1892).
[7] D. G. Archer and R. W. Carter, *J. Phys. Chem. B*, **104,** 8563 (2000).
[8] E. Trinh and R. E. Apfel, *J. Chem. Phys.,* **69**, 4275 (1978).
[9] J. P. Petitet, R. Tufeu, and B. Le Neidre, *Int. J. Thermophys.*, **4,** 35 (1983).
[10] G. S. Kell, *J. Chem. Eng. Data* **20,** 97 (1975).
[11] D. E.Hare and C. M. Sorensen, C. M., *J. Chem. Phys.*, **87**, 4840 (1987).
[12] T. F. Young and W. D. Harkins, in *International Critical Tables*, edited by E. W. Washburn (McGraw-Hill, New York, 1928), vol. IV, p. 446.
[13] Hacker, P. T., Technical Note 2510, National Advisory Committee for Aeronautics (1951).
[14] M. A. Floriano and C. A. Angell, *J. Phys. Chem.,* **94,** 4199 (1990).
[15] K. Röttger, A. Endriss, J. Ihringer, J., S. Doyle, and W. F. Kuhs, *Acta Cryst. B* **50**, 644 (1994).
[16] B.E. Poling, J.M. Prausnitz, J.P. O'Conell, *The Properties of Gases and Liquids*, 5th Ed., McGraw-Hill, New York (2001)
[17] IAPWS Release on Surface Tension of Ordinary Water Substance, IAPWS (1994) http://www.iapws.org/relguide/surf.pdf.
[18] N. B. Vargaftik, B. N. Volkov, and L. D. Voljak, International tables of the surface tension of water. *J. Phys. Chem. Ref. Data,* **12,** 817 (1983).